ON THE REQUIREMENTS FOR MODEL-BASED THERMAL CONTROL OF MELT POOL GEOMETRY IN LASER POWDER BED FUSION ADDITIVE MANUFACTURING

Fox, Jason; Lopez, Felipe; Lane, Brandon; Yeung, Ho; Grantham, Steven

National Institute of Standards and Technology, Gaithersburg, Maryland 20899, United States

Keywords: Powder Bed Fusion, Control, Melt Pool

Abstract

As additive manufacturing processes mature, process control is increasingly sought after as a means for improved quality. Accurate and responsive control of melt pool geometry in laser powder bed fusion processes is expected to improve the final part microstructure, prevent over- and under- melting defects, improve surface finish and mechanical properties, and reduce residual stress. Various approaches for process control of melt pool geometry have been proposed but there are still significant barriers for their adoption. In this paper, we look into the elements of such process controllers and identify their requirements in terms of range of operation and bandwidth; and discuss the feasibility of such control systems.

Introduction

Laser powder bed fusion (L-PBF) additive manufacturing (AM) technologies are used to fabricate solid objects from three-dimensional (3D) model data by fusing selected regions of a powder bed with a laser and repeating the process for every layer [1]. L-PBF is considered one of the most promising AM technologies due to its superior surface and geometric quality, and its capability to work with a wide spectrum of materials. Metallic parts produced with L-PBF AM have been found to be almost fully-dense and to reach mechanical properties that sometimes surpass those of components produced with conventional methods [2]. In spite of all the attention drawn, these processes are still not considered mature. Currently, the inability to guarantee material properties is holding back their adoption as there is no confidence that manufactured parts will meet specific structural needs. Significant effort has been dedicated to the search of predetermined optimal processing conditions to result in desired mechanical properties for a given part. However, this approach is not economical nor robust enough to deal with perturbations.

Process control has been identified as an important area of research in AM and had been considered critical "to achieve predictable and repeatable operations" [3]. Vlasea et al. identified four approaches for monitoring and control in AM: pre-process optimization, in-situ defect detection, feedback control, and signature-derived control [4]. While the first two approaches focus on optimization and monitoring, the last two rely on feedback to identify and mitigate process

perturbations, improving process robustness and repeatability. Perturbations appear frequently in AM processes and are caused either by geometry variations in the vicinity of the melting and solidification front (e.g., overhanging structures), or by variations in external sources (e.g., ambient temperature, particle size distribution). While the former are repeatable and can be identified with repeated experimentation, the latter can only be addressed with feedback.

In spite of the promise held by feedback control methods in AM, significant barriers hinder their adoption. Some of them are: 1) lack of adequate process measurement methods to track thermal and dimensional parameters throughout the build [5], 2) high sampling rates required to capture fast solidification dynamics in metal-based AM [6], and 3) lack of appropriate models for online estimation and control [7]. This paper discusses the identified barriers and outlines the requirements for thermal feedback controllers for melt pool geometry in L-PBF AM. The feasibility for such controllers with current technology is also discussed.

Background

Mani et al. reviewed correlations between process parameters, process signatures, and product qualities in PBF AM of metals [5]. In their review work, three classes of product qualities are identified: geometric (e.g., under- and over-melting defects), mechanical (e.g., strength and fatigue resistance), and physical (e.g., residual stress, porosity, and surface roughness).

The same work also identified a large number of process signatures which may potentially be monitored to identify irregularities that might result in poor product qualities. For instance, under- and over-melting are known to be caused by insufficient or excessive heat deposition on the melt pool, respectively. The former may result in porosity, which is known to have an adverse influence on tensile and fatigue strength [8], while the latter may compromise dimensional accuracy and surface finish [9]. The origin of both kinds of defects may be traced back to melt pool dimensions. Conversely, microstructural characteristics such as grain size and morphology, responsible for yield strength and other mechanical properties [10], and residual stress, known to have a strong influence on fatigue crack growth [11], are dependent on the thermal history during solidification, which is in turn related to melt pool dimensions as well [10, 12].

To improve the three classes of product qualities introduced by Mani et al., it is sufficient to control melt pool dimensions throughout the entire process. Various dimensions can be used as control parameters: surface area, width, length, depth, or cross-sectional area. Among the melt pool feedback controllers found in the literature, most target surface area [13] presumably because it can be measured with non-invasive imaging techniques. Alternatively, among offline approaches, process maps are often used to identify combinations of process parameters yielding constant key quantities, such as melt pool dimensions and microstructure [10, 14, 15].

Two of the approaches identified by Vlasea et al. may be used to ensure stable melt pool geometries throughout the process: feedback control, and signature-derived control [4]. Feedback control allows for the intelligent modulation of process parameters following measurements of process signatures. Feedback control approaches for AM are more often utilized in directed energy deposition processes. Most approaches are based on thermal signals gathered with cameras and photodetectors. The algorithms most often used are based on Proportional-Integral-Derivative

(PID) controllers [13, 16, 17], or more advanced approaches like model predictive control (MPC) [18]. A typical block diagram for a feedback controller is shown in Figure 1a, where the controller reads a reference melt pool parameter and compares it with a measurement. The controller then decides on optimal laser power and speed (or just one input) that are fed to the AM machine, along with a pre-defined scanning trajectory. At the same time, melt pool measurements are gathered from the machine and sent back to the controller, closing the loop.

(a) Feedback control. (b) Signature-derived control.
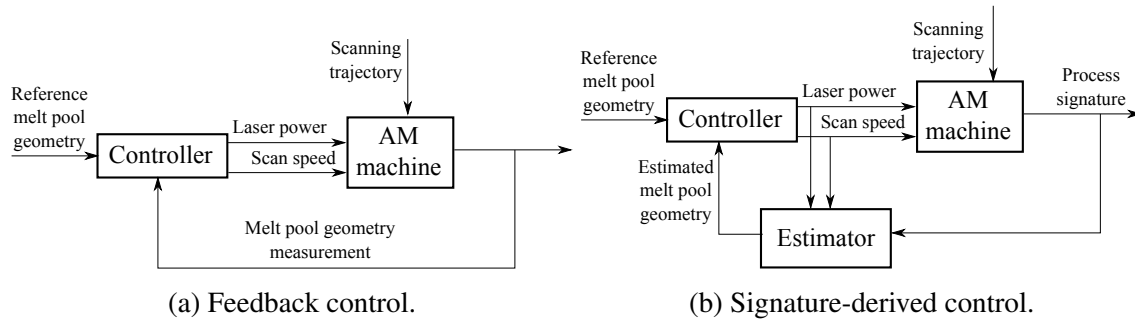
Figure 1: Block diagrams for different types of process control.

Signature-derived control, on the other hand, relies on estimates from process models that use in-situ measurements as inputs to identify quantities that may not be observed directly. These estimates are then fed to the controller to find optimal control inputs to feed to the machine. This approach involves simulations running in parallel to the physical plant or process maps being accessed dynamically. So far, the adoption of these controllers has been hampered by the lack of models to map measurements to thermal signatures, and the fast process dynamics which forces computations to be performed at high speed. A block diagram is shown in Figure 1b, which differs from Figure 1a only in that an estimator is required to process melt pool measurements.

Common elements can be identified from the block diagrams illustrated in Figures 1a and 1b: three blocks (controller, AM machine, and estimator) and various signals (control reference, laser power, scan speed, scanning trajectory, and measured and estimated melt pool geometry). Requirements on resolution and bandwidth are imposed on each element, while controllability and observability conditions need to be met in the system.

Plant model

Control requires knowing how the process will respond to modulation of inputs (laser power and scan speed). The design of process controller may be based on heuristics or on plant models that describe the dynamic relationship between inputs and outputs. In the case of melt pool dynamics, the plant model is expected to describe heat flow in and out of the melt pool region. Plant models for AM have been obtained from first principles [19, 20] and from system identification [2, 13]. Such models are often low-order (as compared to finite element models, for example) because they are required to run faster than the characteristic times of the processes included in the model.

The single requirement from the plant model is that it captures the dynamic evolution of the process output (temperature or intensity measurement in feedback control and melt pool geometry in signature-based control) for changes in process inputs (power and/or speed). However, the plant

model introduces requirements on the bandwidth of other elements in the control system depending on the characteristic times identified in the model. For example, previous work in L-PBF determined that the dynamics of melt pool area had a characteristic time of 1.5 ms for steel processed at 300 mm/s [13]. This prediction can be extended to other materials and scanning speeds following the dimensionless time variable $\tau = \alpha t/L^2$, where α is the thermal diffusivity, t is time, and L is a characteristic length*. Extensions to nickel alloys (processed at higher speeds: 800 mm/s for alloy 625) suggest a characteristic time of 0.15 ms. Then, if the controller sampling time is determined as ten times higher than the characteristic time (common rule of thumb), then a frequency of 60 kHz would be required. The high sampling frequency required for feedback control in L-PBF has already been discussed and the requirement was set to a minimum of 10 kHz [6, 21].

Co-axial melt pool monitoring systems

L-PBF build areas may be on the order of hundreds of mm in length, while melt pools are hundreds of μm. For this reason, staring configurations, where an imager has a stationary view of the build plane, would require hundreds of megapixels to resolve the entire build area with spatial resolution (μm/pixel) on the same order of the melt pool size. In co-axial imaging systems, the imager or detector is optically aligned with the laser beam such that the field of view moves with the laser spot, and the image of the melt pool is split from the laser optical path with a beam-splitter to form a stationary view of the melt pool on the imager. For melt pool monitoring (MPM) systems, the co-axial configuration is more likely to provide adequate spatial resolution to resolve melt pool geometry. In addition to an imager, another beam splitter may be employed to route part of the back-emitted radiation into a photodetector [21, 22], which provides higher temporal bandwidth than an imager [23].

For feedback control, it is sufficient to detect relative changes to the melt pool size. However, co-axial MPM systems will incur measurement uncertainty in spatial, temporal, and overall signal level values. The magnitude of measurement uncertainty ultimately depends on how the melt pool images are processed (e.g., Clijsters et al. defined "melt-pool area" as number of pixels above a threshold value [6]). Figure 2 demonstrates the measurement process chain for a single image.
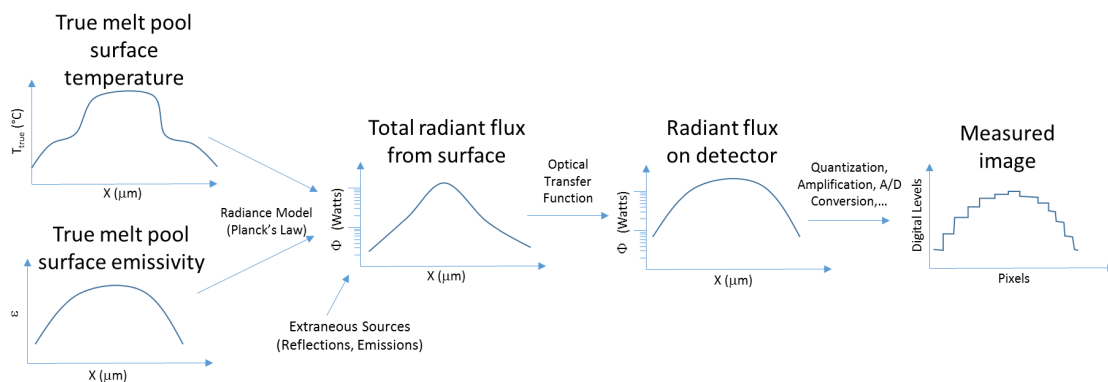
Figure 2: Measurement process chain for determining melt pool size from a thermographic image.

---

*For heat transfer problems with source moving with speed v, $L = 2\alpha/v$.

Each transformation can incur uncertainty in spatial and signal level values. However, analysis of these uncertainties is complex, and not discussed here.

The greatest technical hurdle at this time for co-axial MPM imagers is the tradeoff between spatial resolution and limited data transfer rate. Imagers can transfer at a fixed maximum rate, so in order to increase frame rate, the number of acquired pixels must be reduced, which reduces spatial resolution of the melt pool. For example, Berumen et al. required a 20 pixel × 16 pixel window to achieve 10 kHz frame rate [23]. To resolve a nominally 150 μm image of a melt pool, the system would be limited to fluctuations greater than 7 μm, not considering optical blur.

Another limit to temporal resolution, other than frame rate, is the integration time, as shown in Figure 3. Imagers must integrate the incoming signal over fixed periods (integration periods), which must be shorter than the frame period (inverse of frame rate). For example, at 10 kHz frame rate, the longest integration time allowed would be 0.1 ms. If there are melt pool size fluctuations during the integration time, motion blur will occur which further reduces spatial resolution. For this reason, shorter integration times are optimal, and may be reduced to less than 1 μs. However, this reduces the total integrated signal and thus the measurable dynamic range, which again reduces spatial resolution. The optimal integration time must be determined for each MPM imaging system based on its unique sensitivity.
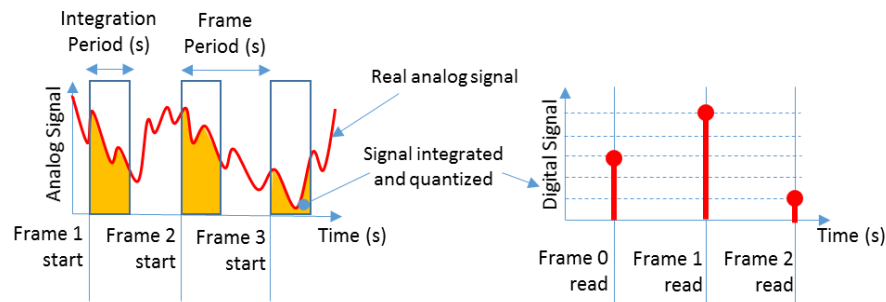
Figure 3: Relationship between frame rate and integration time as limiting factors in temporal resolution for each pixel.

Laser system

The laser beam in L-PBF systems is directed by a pair of mirrors driven by limited rotation direct current (DC) motors optimized for high speed applications, known as galvo motors. These motors are rotated by an electromagnetic force proportional to the current in the motor coils, which is determined by a servo control mechanism with feedback from an internal position encoder attached to the motor shaft. As laser beams are reflected by mirrors, the position on the scan surface is a function of the angular rotation and the laser beam traveling distance (D) from the mirror to the scan surface. For a small rotation (θ in radians), the surface scan distance can be approximated by $D \times \theta$. For example, if $D = 0.4$ m and galvo's full rotation range is $\pm$ 45 degrees for an input voltage of $\pm$ 10V, then 1 mV corresponds to approximately 31.4 μm scan distance when the beam is orthogonal to the surface.
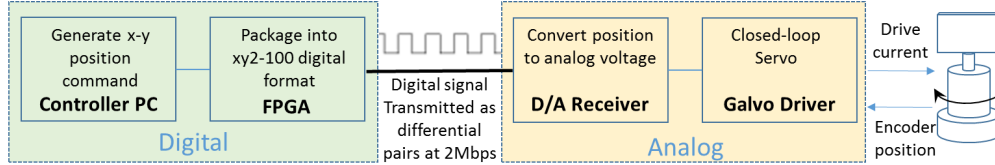
Figure 4: Control system for scan path in NIST AMMT.

Laser control in L-PBF AM consists of two parts: laser power and scan path. Different build strategies can be achieved by their combinations, but are also constrained by their limitations. An example of a field-programmable gate array (FPGA) based control system for a laser scanner is shown in Figure 4. Most commercial L-PBF AM systems have similar designs, but are based on proprietary software/hardware for x-y position generation and packaging motion commands into a standard digital command protocol. Preliminary studies have been conducted on the Additive Manufacturing Metrology Testbed (AMMT) at the National Institute of Standards and Technology (NIST) to characterize the delay between the digital and analog signals (response time) and accuracy of its laser control system. Figure 5 plots a scan of galvo X with acceleration a = 10^8 mm/s^2: $x_{digital}$ is the digital commanded position sent to the D/A receiver, and x_{analog} is the position measured from the galvo driver board. The noise level in x_{analog} is around 50 μm. The x_{analog} peak-to-peak distance is 30 μm less than that for $x_{digital}$, for the $\pm$ 10 mm scan around the neutral position. Note that all measurements were taken in voltage and scaled to distance. The response time was measured to be around 1.15 ms (0.87 kHz), irrespective to the speed profile.
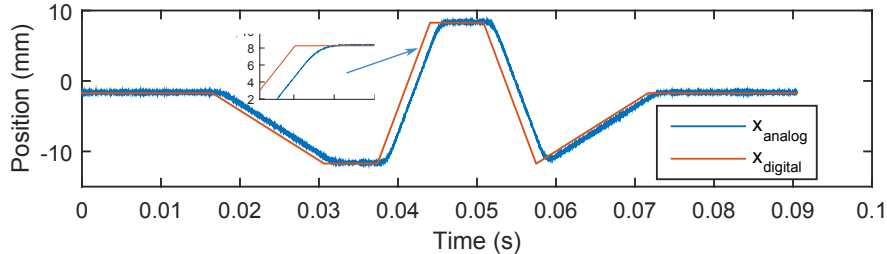
Figure 5: Galvo response for a variable reference.

In the NIST AMMT, the time constant for power adjustment is approximately 50 μs. This quick response would make it possible to adjust power dynamically at a fast rate. Also, the fine resolution of scan position (10 μs micro-step) provides a means to synchronize power perfectly to scan path, suggesting position errors much smaller than 100 μm, the typical laser spot size.

Computational resources

Transfer of data gathered with MPM systems to computational units for post-processing is a slow process. For example, data transfer and loading has been reported to take longer than sampling itself [6]. An approach based on FPGAs to accelerate data transfer for MPM images has been reported [6]. Similar speed requirements are imposed on all transformations and calculations performed on the measurements to return an optimal control signal. Control and estimation need to be performed much faster than the sampling frequency (10 kHz - 60 kHz for nickel alloys).

Currently, calculations are performed on Central Processing Units (CPUs) but they are limited to simple operations (e.g., PID control with no estimation). If more advanced algorithms are to be used, their computational cost must be accounted for, and potentially incorporated in a more adequate computer architecture, as was the case when processing MPM images.

Closing remarks

Table I presents usual bandwidths identified for the control elements discussed in this paper. Controllers for melt pool geometry, as introduced in the background section, require that the collection, transformation, and distribution of data are performed much faster than the characteristic time of the process model (for stability). It should be noted that thermographic imaging barely matches the lower end of the suggested sampling frequency for L-PBF of nickel alloy 625 with nominal conditions. To ensure that MPM is faster than the process itself, one can slow down the process by using slower scanning speeds, or accelerate MPM by using a lower resolution or with the aid of FPGAs. It can also be observed that laser position for typical off-the-shelf galvanometers has too slow a response for online adjustment suggesting that, in real-time control, laser power is more likely to be the manipulated variable while laser position is predefined. Furthermore, data processing (expected to depend on the chosen algorithms and hardware) was not included in this comparison but is expected to impose tighter speed requirements on the system.

Table I: Characteristic frequencies identified for elements of process controllers.

	Sampling	Laser power	MPM	Laser position
Frequency (kHz)	10 - 60	50	5 - 10	0.9

Experimental studies will be necessary to determine the effective observability of the system, defined as how accurately process dynamics can be identified from uncertain measurements. Two factors that can potentially compromise observability are low sampling frequency and measurement uncertainty, which was left out of this discussion. Until a complete study of the requirements on bandwidth and precision is completed, it is not possible to conclude whether accurate control of melt pool geometry in L-PBF can be attained.

As our understanding of the links between observable melt pool signatures and the desired outcomes, such as the resultant part microstructure, continue to mature, so too will the robustness and accuracy of the process. However, while offline approaches and monitoring systems can aid in the qualification or certification that a part meets desired specifications, these methods cannot prevent the failure of a build should unpredictable external sources cause undesired variations in the process. As such, the continued development of feedback control systems will be required to mitigate these variations and maintain process robustness and repeatability.

References

[1] ASTM, "Standard terminology for additive manufacturing technologies" (ASTM F2792)

[2] T. Craeghs, et al., "Feedback control of layerwise laser melting using optical sensors," *Physics Procedia*, 5(B) (2010) 505-514.

[3] National Institute of Standards and Technology, "Measurement science roadmap for metal-based additive manufacturing," (NIST, 2013).

[4] M. Vlasea et al., "Development of a powder bed fusion additive manufacturing testbed for enhanced real-time process control," *Proc. Solid Freeform Fabrication Symposium*, (2015) 527-539.

[5] M. Mani et al., "Measurement science needs for real-time control of additive manufacturing powder bed fusion processes" (NISTIR 8036, NIST, 2015).

[6] S. Clijsters et al., "In situ quality control of the selective laser melting process using a high-speed, real-time melt pool monitoring system," *Int. Journal of Advanced Manufacturing Technology*, 75 (2014), 1089-1101.

[7] F. Verhaeghe et al., "A pragmatic model for selective laser melting with evaporation," *Acta Materialia*, 50 (20) (2009), 6006-6012.

[8] J.P. Kruth et al., "Consolidation phenomena in laser and powder-bed based layered manufacturing," *CIRP Annals-Manufacturing Technology*, 56(2) (2007) 730-759.

[9] K. Mumtaz and N. Hopkinson, "Top surface and side roughness of Inconel 625 parts processed using selective laser melting," *Rapid Prototyping Journal*, 15(2) (2009) 96-103.

[10] J. Gockel, J. Beuth, and K. Taminger, "Integrated control of solidification microstructure and melt pool dimensions in electron beam wire feed additive manufacturing of Ti-6Al-4V," *Additive Manufacturing* 1 (2014) 119-126.

[11] A. Wu et al., "An experimental investigation into Additive Manufacturing-induced residual stresses in 316L Stainless Steel," *Metallurgical and Materials Transactions A*, 45A (13) (2014) 6260-6270.

[12] R. Dehoff et al., "Site specific control of crystallographic grain orientation through electron beam additive manufacturing," *Materials Science and Technology*, 31(8)(2015) 931-938.

[13] J. Kruth et al., "Feedback control of selective laser melting," *Proc. 3rd Conference on Advanced Research in Virtual and Rapid Prototyping*, (2007).

[14] J. Beuth et al., "Process mapping for qualification across multiple direct metal additive manufacturing processes," *Proc. Solid Freeform Fabrication Symposium*, (2013) 655-665.

[15] C. Montgomery et al., "Process Mapping of Inconel 625 in Laser Powder Bed Additive Manufacturing," *Proc. Solid Freeform Fabrication Symposium*, (2015) 1195-1204.

[16] A. Fathi et al., "Clad height control in laser solid freeform fabrication using a feedforward PID controller," *Int. Journal of Advanced Manufacturing Technology*, 35 (2007) 280-292.

[17] D. Salehi and M. Brandt, "Melt pool temperature control using LabVIEW in Nd:YAG laser blow powder cladding process," *Int. Journal of Advanced Manufacturing Technology*, 29 (2006) 273-278.

[18] L. Song et al., "Control of melt pool temperature and deposition height during direct metal deposition process," *Int. Journal of Advanced Manufacturing Technology*, 58 (2012) 247-256.

[19] W. Devesse, D. De Baere, and P. Guillaume, "Design of a model-based controller with temperature feedback for laser cladding," *Physics Procedia*, 56 (2014) 211-219.

[20] P. Sammons, D. Bristow, and R. Landers, "Iterative learning control of bead morphology in laser metal deposition processes," *Proc. of the 2013 American Control Conference*, (2013).

[21] T. Craeghs et al., "Online quality control of selective laser melting," *Proc. Solid Freeform Fabrication Symposium*, (2014) 212-226.

[22] Y. Chivel and I. Smurov, "On-line temperature monitoring in selective laser sintering/melting," *Physics Procedia* 5 (B) (2010) 515-521.

[23] S. Berumen et al., "Quality control of laser- and powder bed-based Additive Manufacturing (AM) technologies," *Physics Procedia* 5 (B) (2010) 617-622.

140